



Development of a microfluidic-assisted open-source 3D bioprinting system (MOS3S) for the engineering of hierarchical tissues

Sajad Mohammadi^{a,b}, Salvatore D'Alessandro^{a,b}, Fabiano Bini^b, Franco Marinozzi^b, Gianluca Cidonio^{a,*}

^a Center for Life Nano & Neuro-science (CLN2S), Istituto Italiano di Tecnologia (IIT), Rome, Italy

^b Department of Mechanical and Aerospace Engineering, Sapienza University, Rome, Italy

ARTICLE INFO

Keywords:

3D-bioprinting
Open-source
Hydrogel
Microfluidic
Tissue Engineering

ABSTRACT

The engineering of new 3D bioprinting approaches has shown great promise in the field of tissue engineering and disease modelling. However, the high cost of commercial 3D bioprinters has limited their accessibility, especially to those laboratories in resource-limited settings. Moreover, the need for a 3D bioprinting system capable of dispensing multiple materials is growing apace. Therefore, the development of a Microfluidic-assisted Open Source 3D bioprinting System (MOS3S) for the engineering of hierarchical tissues is needed to progress in fabricating functional tissues, but with a technology accessible to a wider range of researchers. The MOS3S platform is designed to allow the deposition of biomaterial inks using microfluidic printheads or coaxial nozzles for the *in-situ* cross-linking and scaffolds fabrication. The coupling of 3D printed syringe pumps with the motion control system is used for driving the tunable extrusion of inks for the fabrication of centimeter scale hierarchical lattice constructs for tissue engineering purposes. MOS3S performance have been validated to fabricate high-resolution structures with coaxial microfluidic technology, opening to new frontiers for seminal studies in pre-clinical disease modelling and tissue regeneration.

Specifications table

Hardware name	MOS3S (Microfluidic-assisted Open Source 3D bioprinting System)
Subject area	<ul style="list-style-type: none"> • Engineering and materials science • Educational tools and open-source alternatives to existing • Biological sciences • Biological sample handling and preparation • Mechanical engineering and materials science • 3D printer modification
Hardware type	Aspect Biosystems
Closest commercial analog	GNU General Public License (GPL) v3.0
Open-source license	677 €
Cost of hardware	https://data.mendeley.com/datasets/s8bpwp2ryb/1
Source file repository	(DOI: 10.17632/s8bpwp2ryb.1)

* Corresponding author at: Center for Life Nano & Neuro-science (CLN2S), Istituto Italiano di Tecnologia (IIT), Rome, Italy.

E-mail address: Gianluca.Cidonio@iit.it (G. Cidonio).

@@[gianluccidonio](https://www.instagram.com/gianluccidonio) (G. Cidonio)

<https://doi.org/10.1016/j.ohx.2024.e00527>

Received 25 August 2023; Received in revised form 26 March 2024; Accepted 29 March 2024

Available online 2 April 2024

2468-0672/© 2024 The Authors. Published by Elsevier Ltd. This is an open access article under the CC BY-NC-ND license (<http://creativecommons.org/licenses/by-nc-nd/4.0/>).

1. Hardware in context

Additive manufacturing (AM) is a fabrication process based on the subsequent layering of materials to generate three-dimensional structures based on a computer-aided design (CAD). AM is offering a number of advantages over canonical fabrication methodologies, such as a fast production process of prototypes and reduced waste of deposited materials [1]. Today, a number of 3D printers are available at a convenient price, enabling researchers to investigate the potential of this technology in different fields of study and research. A wide spectrum of applications can be mentioned for 3D printing, from aviation, jewelry, and sculpture to the food [2] and healthcare industry [3]. Recently, the ability of AM in fabricating biologically-relevant structures has captured the interest of engineers and biologists, who have come together to foster the development of 3D bioprinting for tissue fabrication [4] and disease modelling purposes [5,6].

3D bioprinting is a biofabrication technique that utilizes a combination of biomaterials, living cells, and other bioactive compounds such as drugs and growth factors, to generate constructs that mimic the appearance and function of natural tissues.

To date, jetting-based bioprinting, laser-induced forward transfer (LIFT), extrusion-based bioprinting (EBB) and vat photopolymerization-based bioprinting [7] are the most common platforms currently used to fabricate tissue substitutes [8]. Although delving into the pros and cons of these techniques is beyond the scope of this paper, it is noteworthy to mention that EBB is the most commonly used technique in fabricating cell-laden scaffolds. EBB has enabled the researchers to deposit a wide range of hydrogels of varying viscosities, as well as high cell density; though the resolution of the printed structures is limited to the range of 200–1000 μm [9]. Besides, the EBB method could impose extreme conditions such as high pressure and shear stress on the encapsulated cells, making it detrimental for fabricating cell-laden hydrogels [5,10]. Moreover, EBB is currently limited in the printing complexity, resulting capable of generating structures with a single material ink at-a-time [11]. Multi-material 3D bioprinters have been assembled, but the complexity of the hardware and the repetitive printhead changes are inconvenient and challenging to engineer.

To this end, microfluidic-assisted 3D bioprinting is coming to the fore, with the capability to address the afore-mentioned challenges by providing precise control over the extrusion of low-viscosity hydrogels, hierarchical patterning of biomaterials, and handling multi-material in inlet with a single controlled fiber at the outlet [12,13]. In this regard, the development of coaxial extruders has attracted recent interest since this strategy offers high deposition resolution with remarkable precision. The working principle involves the delivering of material ink and cross-linking agent through the inner (core) and outermost (sheath) nozzle, respectively [14–16], offering an evident advantage over EBB platforms in the generation and control over bioprinted fibers. To the best of our knowledge, a microfluidic-assisted 3D bioprinting platform has never been released as an open-source assembly.

To date, 3D bioprinting systems are sold at an exorbitant cost, significantly reducing further development of this technology [17]. Additionally, the majority of commercially available 3D bioprinters are manufactured with limited customization options both in hardware and software, greatly impairing the possibility to adapt the AM system to the required clinical application [18]. Lastly, the set of skills and training required to operate and maintain the 3D bioprinting apparatus, as well as high-cost consumable equipment, are further great limitations for the use of AM technologies applied to tissue engineering and regenerative medicine purposes. Thus, a considerable effort has been recently focused on the engineering of a Microfluidic Open Source 3D bioprinting System (MOS3S) that result simple to use and set up [19,20]. Recently, a number of attempts have been spent on assembling single ink extrusion [11], free-form [21], multi-syringes [22], FDM, and syringe dispenser [17]. Considering the tremendous effort spent to design more accessible 3D bioprinting systems, the platforms engineered so far are not up to the standards of commercial 3D bioprinters in terms of printability

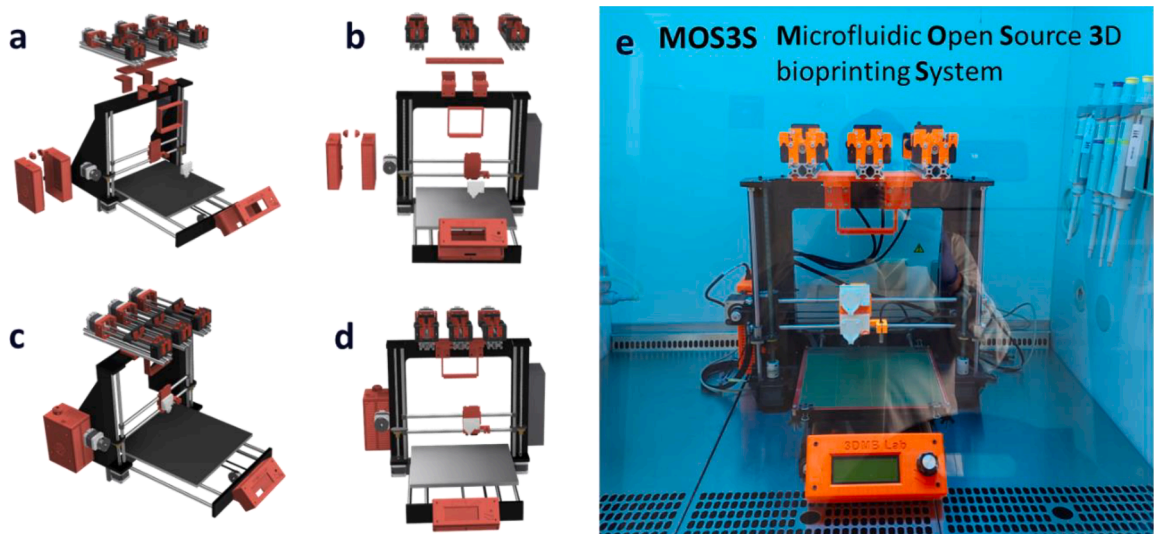


Fig. 1. Render imaging of the developed 3D bioprinter: (a) side view of exploded, (b) front view of exploded, (c) side view of assembled, (d) front view of assembled and (e) Microfluidic 3D bioprinter, equipped with three 3D printed syringe pumps, housed in a sterile cell culture hood (class II).


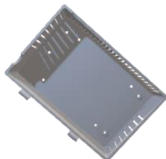

Table 1

The following parts are designed using Computer Aided software (CAD) and manufactured by FDM 3D printer to be assemble and create the microfluidic 3D bioprinter.

Design file name	Render image	File type	Open source license	Location of the file
End motor support		STL	GPLv3	10.17632/s8bpwp2ryb.1
Clamp syringe pump		STL	GPLv3	10.17632/s8bpwp2ryb.1
End idler		STL	GPLv3	10.17632/s8bpwp2ryb.1
Carrier		STL	GPLv3	10.17632/s8bpwp2ryb.1
Clamp plunger retainer		STL	GPLv3	10.17632/s8bpwp2ryb.1
Syringe support 1		STL	GPLv3	10.17632/s8bpwp2ryb.1
Syringe support 2		STL	GPLv3	10.17632/s8bpwp2ryb.1
X-axis carriage		STL	GPLv3	10.17632/s8bpwp2ryb.1
Platform holder		STL	GPLv3	10.17632/s8bpwp2ryb.1
Display box 1		STL	GPLv3	10.17632/s8bpwp2ryb.1
Display box 2		STL	GPLv3	10.17632/s8bpwp2ryb.1

(continued on next page)

Table 1 (continued)

Design file name	Render image	File type	Open source license	Location of the file
Cable & electronic box 1		STL	GPLv3	10.17632/s8bpwp2ryb.1
Cable & electronic box 2		STL	GPLv3	10.17632/s8bpwp2ryb.1
Cable & electronic box 3		STL	GPLv3	10.17632/s8bpwp2ryb.1

and resolution. Moreover, the custom systems are still limited in the materials and technology they can process, with yet poor adjustability and range of tissue engineering applications.

In this work, we aim to engineer a unique 3D microfluidic-assisted extrusion-based bioprinter (MOS3S) combining a modified low-cost desktop FDM 3D printer with custom open-source syringe pump tools to provide a new syringe-based 3D bioprinter for the dispensing of low-viscosity hydrogels. The 3D bioprinting platform has been designed with a plug-and-play system capable of hosting multiple microfluidic printheads and ultimately capable of generating three-dimensional gradients with high-end dispensing, deposition accuracy and resolution.

2. Hardware description

The MOS3S microfluidic-assisted extrusion-based 3D bioprinter (Fig. 1) has been developed starting from a low-cost *Geetech Pro I3 B* as a FDM 3D printer. The 3D printer was initially capable of printing thermoplastic filaments, such as PLA and PETG, at elevated temperature (210 °C and 250 °C, respectively), but further modified for syringe-guided extrusion with microliter resolution.

In this work, the printhead has been removed to house a custom 3D printed platform holding an adjustable microfluidic chip and coaxial nozzle holder. The new development has allowed the printer to deposit *in-situ* cross-linked low-viscosity hydrogels, using installed syringe pumps. The printer is equipped with Rumba board and GT2560 to control the printhead and syringe pumps, respectively. Both main boards are all-in-one electronic, feature an onboard low-power, high-performance 8-bit ATmega 2560 microcontroller. The linear motion mechanics in the custom 3D printed syringe pumps enables the piston of a disposable syringe to be controlled. This mechanism is moved by a stepper motor, stepper driver, and the firmware uploaded into the electronic main boards to guide the material deposition, as well as printhead movements. The MOS3S bioprinter demonstrates significant accuracy, to minimize the waste by means of extruding controlled amount of material inks in a controlled and guided manner. Thus, MOS3S is ultimately found capable of dispensing multiple materials in a graded fashion allowing to recapitulate complex architectures with reproducible and controllable procedures.

The engineering of the MOS3S with the conversion of the original FDM 3D printer involved a series of steps as follows:

1. The design, 3D printing and assembly of syringe pumps including plastic and mechanical components.
2. The assembly of the syringe pumps and the coupling on the designed supports with the 3D bioprinter.
3. The installation of the electronic hardware modified to operate the 3D bioprinter and the syringe pumps simultaneously.
4. The implementation of the modification needed to adapt the Marlin firmware to command the new main boards and extra syringe pumps of the microfluidic 3D bioprinter.
5. The investigation of the material delivery accuracy and 3D bioprinting resolution

In summary, MOS3S provides following features to the researchers in the biomedical field:

- Extremely low-cost 3D bioprinter compared to commercially available devices.
- Ease of design and assembly, making it accessible to a wide range of research groups.
- Availability for further implementations.
- Significant accuracy for the printing lattice scaffolds and delivering multi-materials with the ability to pattern gradient structures.
- *In-situ* cross-linking of the low-viscosity hydrogels with a coaxial nozzle.

3. Design files summary

Table 1 indicates all the design files with rendered images, necessary to assemble the 3D microfluidic bioprinter. The function and repository location of each component has been briefly listed in Table 1.

Inspired by the open-source syringe pump project and remixes, we have re-designed and implemented a new fully-3D printed syringe pump. The parts of the syringe pump and the modified 3D printer are briefly described below to aid the assembling process.

3.1. End motor support

End motor support is used to attach the NEMA 17 stepper motor, utilizing four $M3 \times 20$ screws. The end motor support is also equipped with two holes to insert the metal rods, connecting the upper part of the syringe pumps to the lower section. This component is further installed on the aluminum rail support with two $M3 \times 15$ screws.

3.2. Clamp syringe pump

Clamp syringe pump is a single CAD file design but needs to be printed three times for each syringe pump. The clamp syringe pump is attached the end-idler with four $M3 \times 40$ screws and two miniature ball bearings, serving as a support to hold the syringe.

3.3. End-idler

The end-idler is connected to the clamps. Using two holes on the sides, the metal rods are inserted and connect the upper and lower part together. These metal rods ensure the linear movement of the syringe plunger.

3.4. Carrier

The carrier is another essential part to be used to transfer the linear movement of the stepper motor to the syringe and ultimately provide injection of the ink. To this end, the clamp plunger retainer is mounted on the carrier to serve as a support for holding the syringe plunger.

3.5. Clamp plunger retainer

Clamp plunger retainer is designed to hold and transfer the linear motion of the stepper motor and leadscrew to the plunger. By pressing the plunger, then the hydrogel is going to be extruded, shaping the desired structure on the surface.

3.6. Syringe support

The syringe support is providing a home for syringes to be mounted onto the 3D printer. It is composed of two horizontal and four L-shaped CAD files to be printed and installed by replacing the LCD.

3.7. X-axis carriage

X-axis carriage has been modified and 3D printed to house a LEGO®-like pin support to offer quick and easy replacement and attachment of the microfluidic printheads.

3.8. Display box

Display box composed of two separated pieces, connected using male to female lock. The LCD is placed in the display box and mounted in front of the heat bed.

3.9. Cable and electronic box

Like the display box, the cable box is printed as a three components part and assembled with M3 screws at the hinges. The cable box is housing the two main boards.

4. Bill of materials summary

Table 2 lists all commercially available components required for the construction of the microfluidic 3D bioprinter. The construction can be divided in different steps, starting from assembly of the syringe pumps and 3D printed parts and, modification in electronics by adding another main board and ultimately uploading the edited firmware to control both syringe pumps the printhead.

Table 2

The following parts are commercially available and were purchased from specific suppliers.

Designator	Component	Number	Cost per unit (€)	Total cost (€)	Source of materials	Material type
Syringe pump	Nema 17 stepper motor	3	31.11	93.33	https://www.dhm-online.com/nema-17/10492-42byghw817-x1-17a-18-motore-passo-passo-stepper-wantai-nema-17-con-connettore.html	Metal, semiconductor, magnet
Syringe pump	5 mm leadscrew	3 × 20 cm	36.41 × 1 m	36.41	https://it.rs-online.com/web/p/barre-filettate/0280385?gb=b	Metal
Syringe pump	8 mm smooth rod	6 × 20 cm	14,14 × 1 m	24.28	https://it.rs-online.com/web/p/barre-metalliche/4377073?gb=b	Metal
Syringe pump	5 mm coupling	3	3.45	10.35	https://www.dhm-online.com/en/flexible-joints/441-flexible-shaft-coupling-55-mm.html	Metal
Syringe pump	8 mm ball bearing	6	2.6	15.6	https://www.dhm-online.com/en/linear-bushings-closed/292-linear-bushings-single-lm6uu.html	Metal
Syringe pump	Miniature ball bearing	6	1.8	10.80	https://www.dhm-online.com/en/3d-printing/1143-2-pieces-radial-ball-bearing-625-zz-ball-bearings-625zz-5165mm-reprap-3d.html	Metal
Syringe pump	Aluminum rail support 20 × 40 × 250	3	5.17	15.51	https://www.dhm-online.com/en/series-5-slot-6/3849-235260-series-5-slot-6mm-cut-to-measure-structural-profiles-anodized-extruded-aluminum-profiles.html#/477-grooved_faces-4_sides_hollow/483-6mm_hollow_structural_profile_5_series-20x40	Metal
Syringe pump	M3 × 10 screws	12	0.33	4.00	https://ie.rs-online.com/web/p/socket-screws/7976266?gb=s	Metal
Syringe pump	M3 × 15 screws	6	0.11	0.66	https://ie.rs-online.com/web/p/socket-screws/8229063?gb=b	Metal
Syringe pump	M3 × 20 screws	12	0.40	4.80	https://ie.rs-online.com/web/p/socket-screws/0293319	Metal
Syringe pump	M3 × 30 screws	6	0.46	2.76	https://ie.rs-online.com/web/p/socket-screws/0293331?gb=s	Metal
Syringe pump	M3 × 40 screws	12	0.29	3.48	https://ie.rs-online.com/web/c/fasteners-fixings/screws-bolts/socket-screws/?searchType=CATCH_ALL_DEFAULT&applied-dimensions=4294881158,4294885793	Metal
Syringe pump	M3 nuts	24	0.02	0.48	https://ie.rs-online.com/web/p/hex-nuts/0560293?gb=s	Metal
Syringe pump	M3 T-Nut Groove 5 mm	12	1.28	15.36	https://ie.rs-online.com/web/p/connecting-components/1809102?gb=s	Metal
Syringe pump and bioprinter	Thermoplastic Filament	1	29.99	29.99	https://www.prusa3d.com/it/prodotto/prusament-pla-jet-black-1kg/	PLA
Electronic control	Rumba board	1	118	118	https://www.dhm-online.com/schede-di-controllo/522-rumba-controller-ramps-14-integrato-mega2560-a4988-3d-printer-reprap.html	Semiconductor
Electronic control	A4988 stepper driver	3	3.9	11.7	https://www.dhm-online.com/driver-per-motori/497-stepper-motor-driver-a4988-red-dissipatore-radiatore-driver-nema-17-reprap.html	Metal, semiconductor
Electronic control	DRV8825 stepper driver	4	4.9	19.6	https://www.dhm-online.com/driver-per-motori/498-drv8825-driver-stepper-motor-ramps-14-reprap-prusa-stepstick-3d-printer.html	Metal, semiconductor
Printhead Z height	PINDA probe	1	25.99	25.99	https://www.prusa3d.com/it/prodotto/superpinda/	Sensor
New component assembly	M4 × 20	8	0.46	3.68	https://it.rs-online.com/web/p/viti-a-brugola/0290102	Metal
	M3 × 25	4	0.49	1.96	https://it.rs-online.com/web/p/viti-a-brugola/0293325	
	M3 × 16	4	0.28	1.12	https://uk.rs-online.com/web/p/socket-screws/0281013	
	M3 × 12	10	0.36	3.6	https://it.rs-online.com/web/p/viti-a-brugola/0281007	
	M3 × 10	12	0.33	4.00	https://ie.rs-online.com/web/p/socket-screws/7976266?gb=s	
	M3 × 10	12	0.33	4.00	https://ie.rs-online.com/web/p/socket-screws/7976266?gb=s	
	M3 × 6	12	0.35	4.2	https://it.rs-online.com/web/p/viti-a-brugola/0280981	
	M4 nut	8	0.06	0.48	https://uk.rs-online.com/web/p/hex-nuts/0189579	
	M3 nut	28	0.02	0.56	https://ie.rs-online.com/web/p/hex-nuts/0560293?gb=s	
	3M T-Nut Groove 5 mm	12	1.28	10.24	https://ie.rs-online.com/web/p/connecting-components/1809102?gb=s	
Total:				477.33 €		

5. Build instructions

The majority of parts use to assemble the 3D microfluidic bioprinter are made from 3D printed PLA filament. All components are recommended to be printed with 20 % infill and 0.2 mm layer height. The assembly of MOS3S starts by assembling the syringe pumps, which can be later installed on the aluminum rail support and onto the 3D bioprinter. All the required components for the syringe pump assembly are shown in Fig. 2. Therefore, the instruction will start from this step as follows:

5.1. Syringe pump assembly

The syringe pump assembly begins from attaching the NEMA 17 stepper motor to the end motor support, using four $M3 \times 20$ screws (Fig. 3).

To assemble the syringe holder portion of the syringe pump (Fig. 4), clamp syringe pumps, end idler, miniature bearing, $M3 \times 40$ screws and nuts are used. First, the nuts are placed into the holes of the syringe clamp and miniature bearings inserted into the middle holes designed to pass the leadscrew. The previously explained clamp should be placed on top and the other two go together in the bottom. Using four 40 mm long M3 screws, all components can be assembled.

The center part plays a crucial role in transferring the linear movement of the stepper motor to the syringe. This part includes two ball bearings which go through the designed place to insert the smooth rods and the clamp to retain the syringe plunger. After inserting the ball bearings, the clamp is screwed up with two 10 mm long M3 screws to the carriage (Fig. 5).

Following the assembly of these parts, the core of the syringe pump can be ultimate (Fig. 6). Therefore, an M3 hexagon nut is inserted into the carriage. Subsequently, the 8 mm coupling can be attached to the stepper motor from one side and to the leadscrew from another side. The screws on the coupling can then be tightened. Ultimately, the leadscrew is mounted through the carriage to form the motion transformation system.

To complete the syringe pumps, two smooth rods should be inserted into the side holes in the end motor support, carriage, and the end idler. In this regard, four nuts are introduced in the holes indicated by yellow arrows on the end motor support and end idler. The smooth rods were then attached to the before mentioned parts and the screws are tightened to avoid further movement and instability (Fig. 7).

Eventually, the syringe should be assembled on the aluminum support (Fig. 8). Post assembly nuts are inserted into the aluminum support's grooves and 15 mm long M3 screws are used to attach the end motor support to the rail. Similarly, the $M3 \times 30$ screws used to secure the attachment of the lower part of the syringe pump.

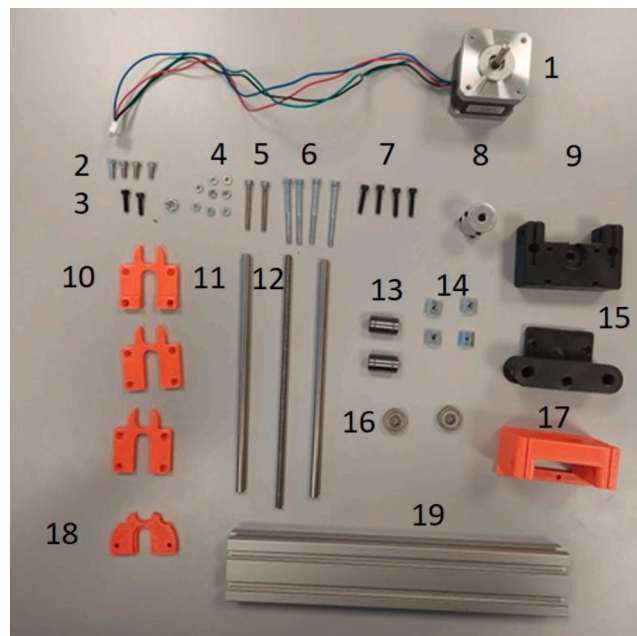


Fig. 2. Required components for syringe pump assembly. 1- NEMA 17 stepper motor, 2 - $M3 \times 10$ screw, 3- $M3 \times 15$ screw, 4 - $M3$ nuts, 5- $M3 \times 30$ screw, 6- $M3 \times 40$ screw, 7- $M3 \times 20$ screw, 8- 8 mm coupling, 9- End-idler, 10- Clamp-syringe pump, 11-20 cm 8 mm Leadscrew, 12-20 cm 8 mm smooth rod, 13-8 mm Ball bearing, 14- $M3$ post-assembly nuts, 15- Carriage, 16- Miniature ball bearing, 17- End motor support, 18- Clamp- plunger retainer, 19- Aluminum rail support.

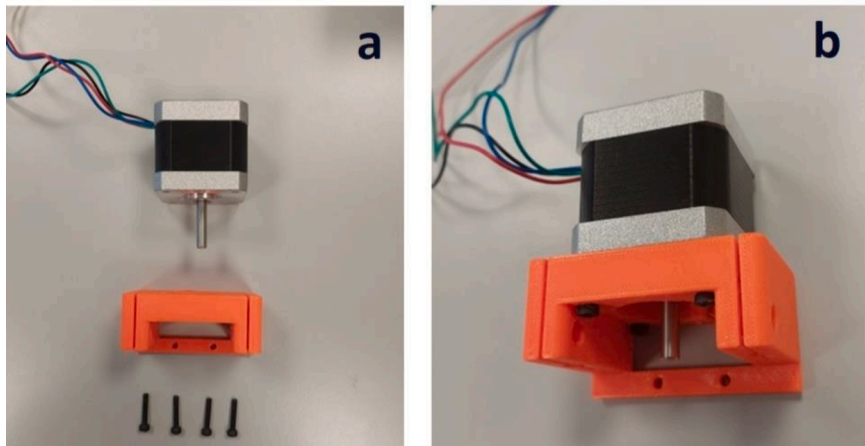


Fig. 3. Assembly of the NEMA 17 stepper motor to the end motor support. (a) Exploded view of the required components (b) assembly.

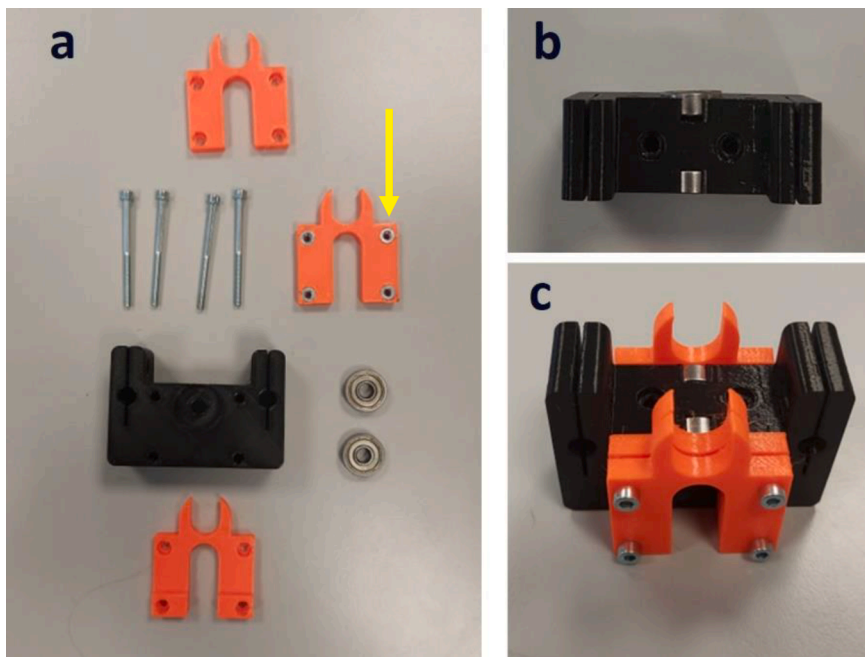


Fig. 4. Lower part of the syringe pump assembly. (a) Exploded view of the components. (b) Miniature bearings were installed before the assembly with (c) syringe holders.

5.2. Coupling syringe pumps with the 3D bioprinter

Following the assembly of the three syringe pumps (Fig. 9a), the coupling with the 3D bioprinter can be implemented. We engineered a custom 3D printed support (Fig. 9b) for the syringe pumps to be located. The pumps are required to be positioned in a direction which minimizes the formation of bubbles, while optimal force is applied to inject the hydrogel (Fig. 9c). Therefore, we assumed the best place to be located would be the top of the built (Fig. 9d), allowing the syringes to be horizontally oriented. Initially, the LCD is dismantled and relocated. The syringe supports are attached to the acrylic body of the printer, using the L-shaped syringe support components and 12 mm long M3 screws and nuts (Fig. 9e,f). The syringe pumps are then mounted on the syringe supports through the grooves of the aluminum rail support and tightened up using $M3 \times 10$ screws and post assembly nut (Fig. 9g).

5.3. X-carriage and platform holder

The X-carriage holder carriage is equipped with grooves for the belt and bearings which ensures smooth movement during the

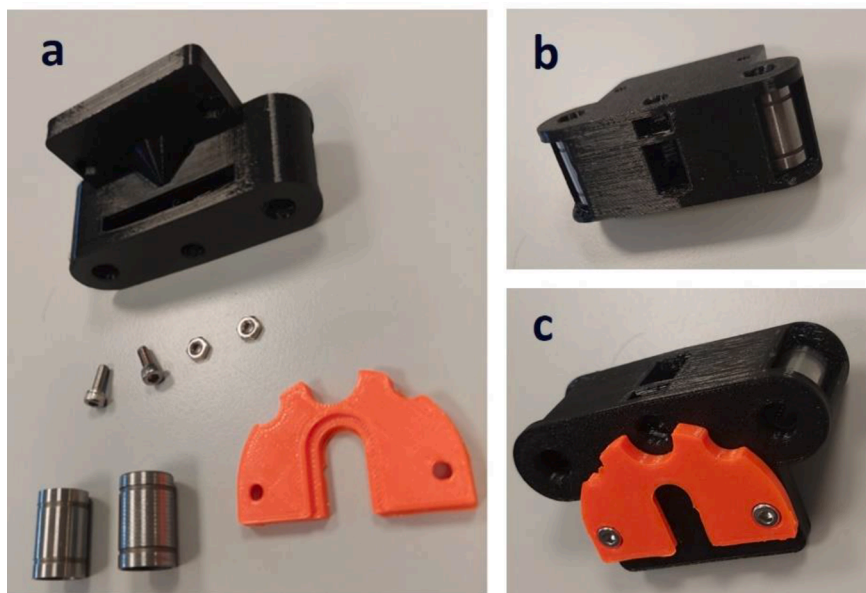


Fig. 5. Setting up the carriage for transferring linear motion to the syringe: (a) Exploded view of the components. (b) ball bearings were installed in the carriage. (c) The clamp syringe retainer attached to the carriage.

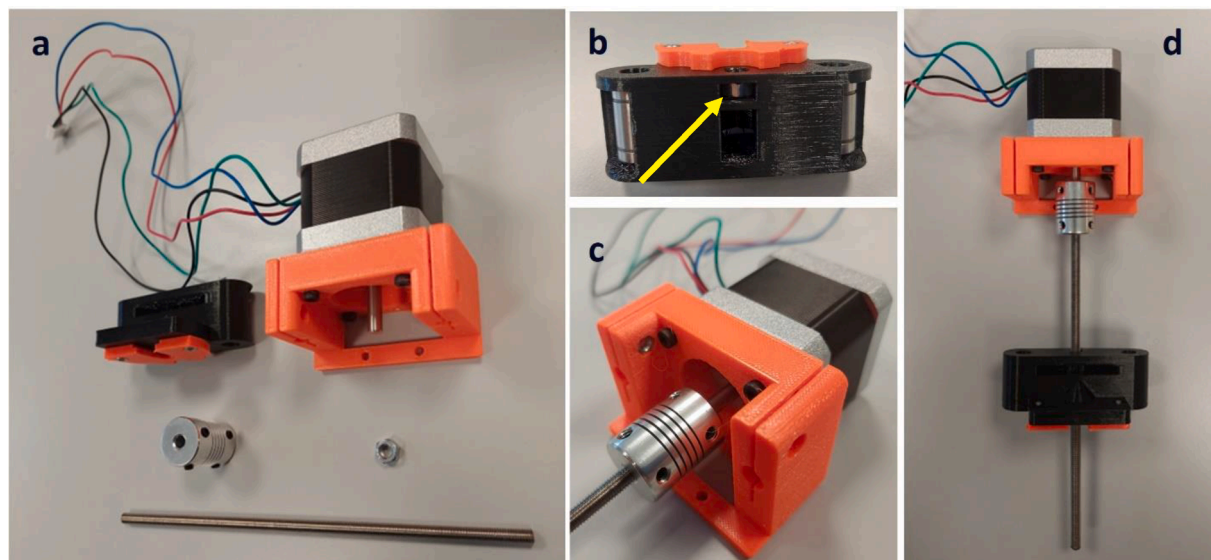


Fig. 6. Construction of the motion transformation parts: (a) Exploded view of the required parts. (b) The hexagon nut is inserted into the carriage. (c) The coupling is installed to the NEMA 17 stepper motor. (d) Top view of the motion transformation section.

deposition process (Fig. 10a,b). This component has been designed in the form of a LEGO®-like platform, with pins equally spaced to match the pattern engraved in the microfluidic printhead support, for easy installation and removal (Fig. 10c,d). The carriage can be mounted on the pre-installed bearings on the smooth rods. The X-carriage is attached to the long bearing using zip ties. Then the belt is inserted into the grooves using a screwdriver to push the belt. Subsequently M3 × 10 screws are used to tighten the black plastic part and the X-carriage together and the zip ties have been trimmed. A side allocated holder has been designed, enabling the carriage to

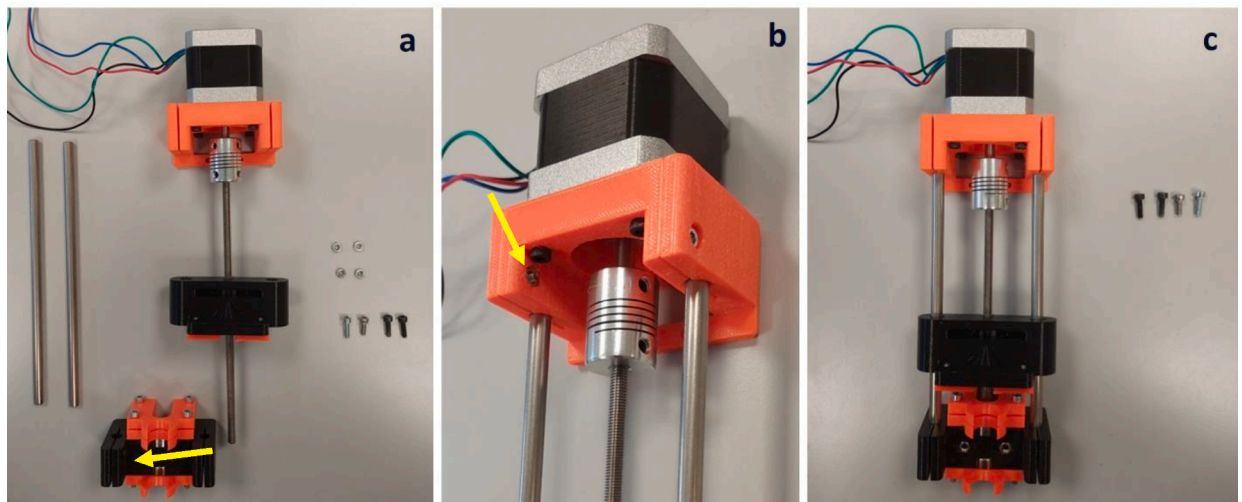


Fig. 7. Mounting the syringe pumps using the side smooth rods: (a) Exploded view of the components. (b) The smooth rods are introduced to the end motor supports and tightened with screws. (c) Top view of the syringe pumps before assembly on the aluminum support.

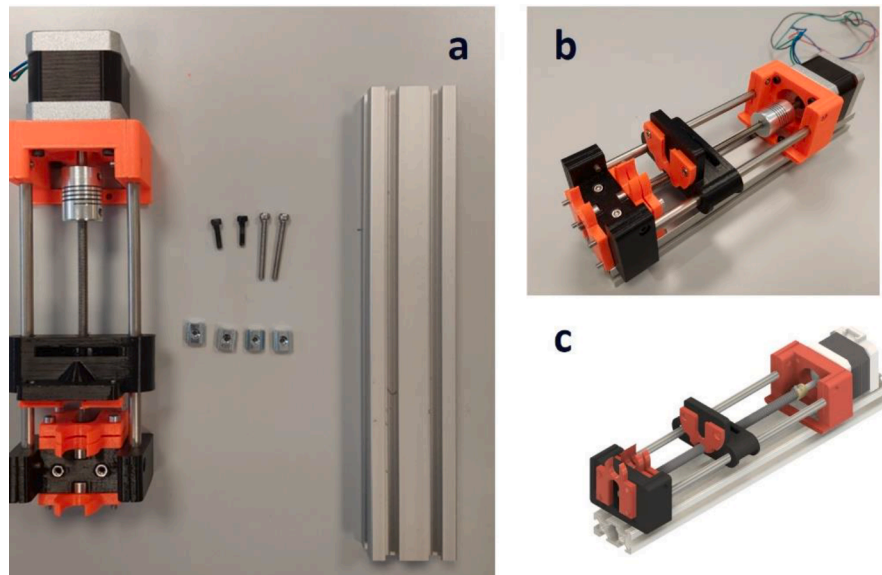


Fig. 8. Assembly of the syringe pump to the aluminum rail support: (a) Exploded view of the essential parts. (b) Attached syringe pump on the aluminum rail support using post assembly nuts. (c) Rendering image of the syringe pump.

hold a PINDA probe for accurate z-height adjustment. Z-offset is the distance between the heat bed and the Z home position. Typically, commercially available FDM 3D printers such as Geetech i3 Pro B, control the Z height by mechanical end stops. However, in this project, we substituted the mechanical end stop for Z-axis, with a proximity sensor probe (PINDA probe). Proximity sensors work by detecting changes in capacitance between the sensor tip and metal objects. Therefore, the glass bed of the printer was replaced with a metal plate (Fig. 10e).

5.4. Display box and LCD

The LCD panel is mounted in the front-lower portion of the 3D biprinter for ease access. The custom LCD box is fixed to the frame using 16 mm long M3 screws and nuts. The second piece is then connected through the hinges and the whole box mounted to the acrylic body of the 3D printer, in front of the heat bed (Fig. 11).

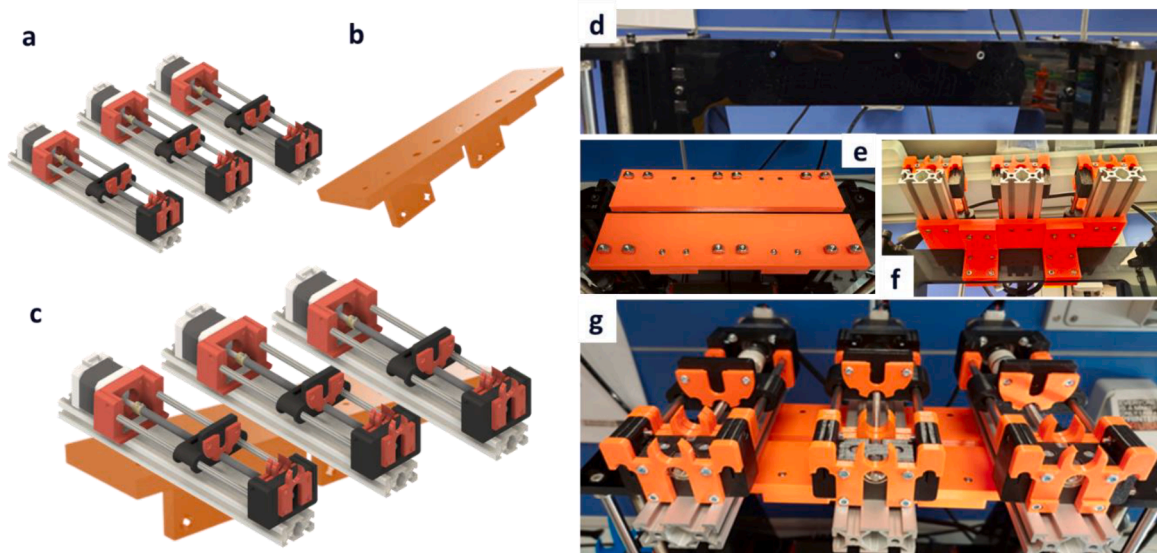


Fig. 9. Assembly of the syringe pumps on the printer: (a) Render images of the syringe pumps. (b) Engineered support to house the syringe pumps. (c) Render images of the assembly. (d) Detaching the display to create space for the syringe pumps. (e) The engineered supports are installed on the top of the printer to house the syringe pumps. (f) Bottom view of the syringe horizontal and vertical syringe supports. (g) Top view of the installed syringe pumps on the 3D bioprinter.

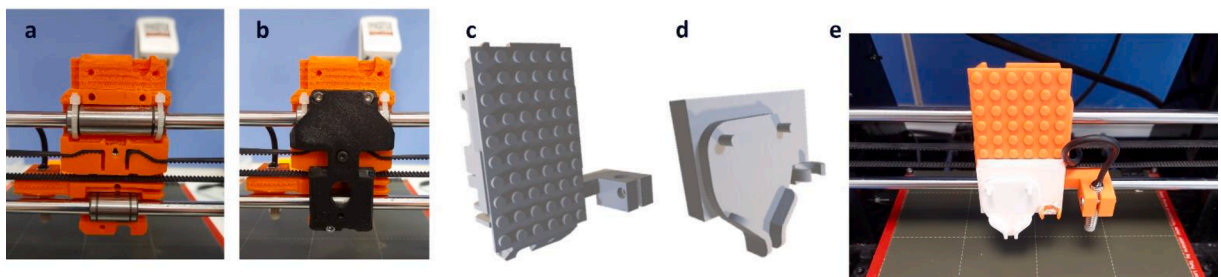


Fig. 10. Construction and assembly of the X-carriage, platform holder and PINDA probe sensor: (a) X-carriage is attached to the smooth rods towards the bearing and the belt is inserted into the grooves. (b) Fixation of the X-carriage using M3 × 10 screws. (c) Render imaging of the X-carriage and (d) platform holder to house the nozzle. (e) Completed X-carriage and attached platform holder, equipped with PINDA probe sensor for Z-height calibration.



Fig. 11. Relocating the LCD by introducing the display box to new spot: (a) Render imaging of the new display box. (b) Top view of the installed LCD to the 3D bioprinter. (c) Front view of the LCD, attached to the acrylic body.

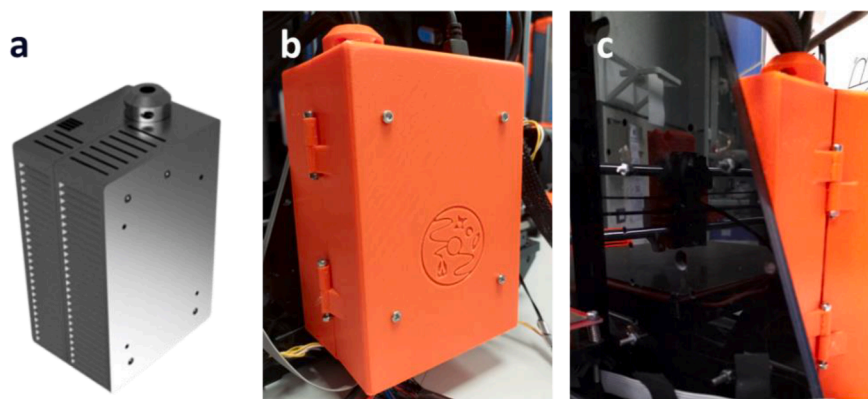


Fig. 12. Mounting the cable and electronic box to the acrylic body of the 3D printer: (a) Render image of the newly designed box for cables and electronic main boards. (b) and (c) Installed cable box to the 3D bioprinter.

5.5. Cable and electronic box

The cable and electronic box (Fig. 12) is used to hold and organize the cables passing from the components to the main boards. The box also houses the electronic main boards. As introduced before, this box is designed in two pieces, connected with two M3 \times 30 screws and nuts. Subsequently, 12 mm long M3 screws are used to mount the cable box to the acrylic body.

5.6. Electronic board and wiring

The Prusa i3 pro B 3D printer originally comes with a GT2560 main board. However, this board does not have enough pins to integrate the PINDA probe. Therefore, the GT2560 board is replaced with a Rumba board to control the injection of the syringe pumps and printer movement, respectively. First, the original board is dismantled and both electronic main boards are located in the cable and electronic box and screwed up with M3 \times 10 screws to new position as showed in Fig. 13a. Subsequently, the DRV8825 and A4988 stepper drivers are installed on the specific place of and Rumba (Fig. 13b) and GT 2560 (Fig. 13c) boards, respectively. Since the system is going to deal with hydrogels and there is no need to increase the temperature of the nozzle to melt the filament, some slots such as heater, fans, thermistor and the filament sensor remain unplugged. Fig. 14 and Fig. 15 provide information on the wiring instruction.

5.7. Firmware modification

All activities of the 3D bioprinter are managed by firmware flashed on the main board. This firmware coordinates all the components involved in the 3D bioprinting procedure, such as printhead movement, plate movement, LCD display, and sensors. In the development of the microfluidic 3D bioprinting system, we modified the Marlin firmware (under GPLv3 License) in the *configuration* file [23]. As an example of firmware modification, changes in E factors can be noted since the stepper drivers are changed. Although

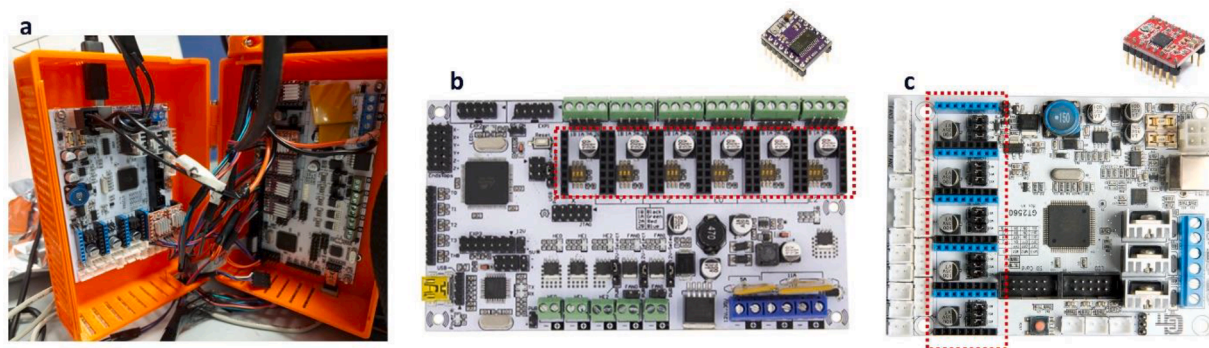


Fig. 13. Assembly of the electronic boards in the cable box (a), Rumba board and DRV8825 stepper drivers (b), GT2560 and A4988 stepper drivers (c).

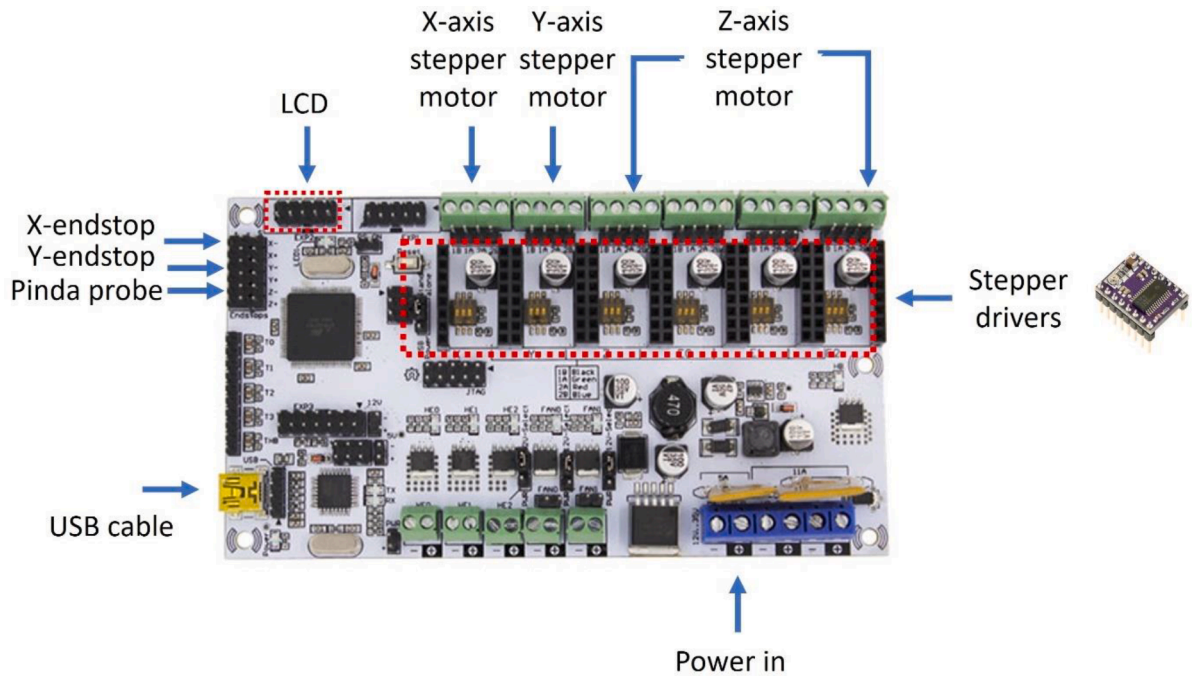


Fig. 14. Wiring instruction for Rumba board, indicating the appropriate slot for the stepper drivers, each axis, End-stops, PINDA probe, LCD, USB cable and power in.

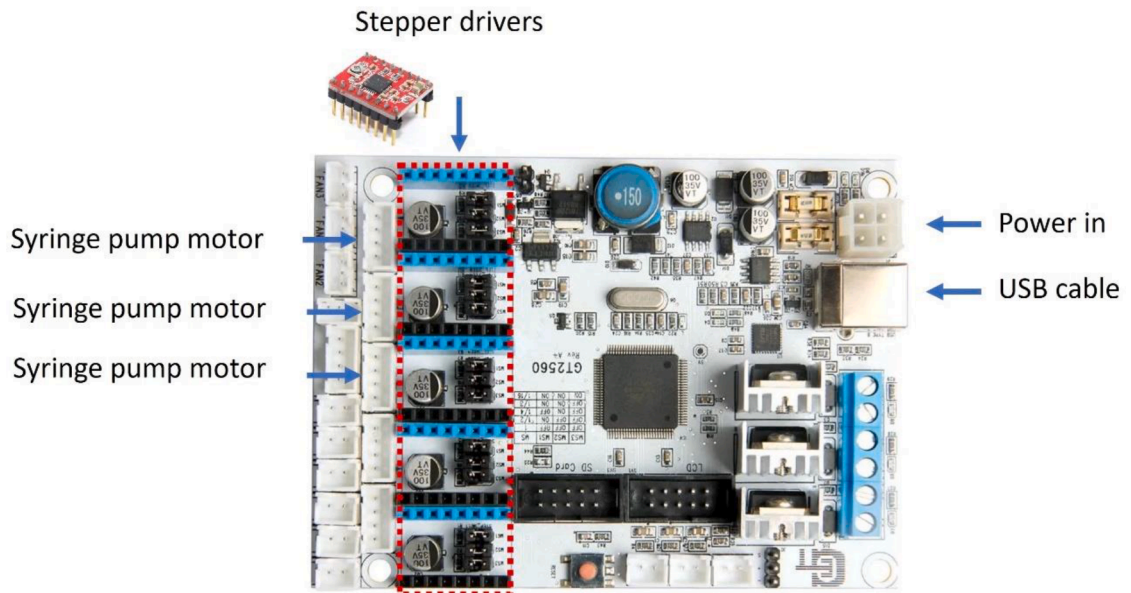


Fig. 15. Wiring instruction for GT2560 board, showing the slots for the power supply, USB connection to PC, stepper drivers and stepper motors.

the full version of the changed firmware for both printhead and the syringe pumps is provided alongside the paper (doi: 10.17632/s8bwpw2ryb.1), here some examples of the modification are mentioned:

Modification for Rumba board:

```
#ifndef MOTHERBOARD
#define MOTHERBOARD BOARD_RUMBA
#endif
#define BAUDRATE 115200
Stepper drivers:
#define X_DRIVER_TYPE DRV8825
#define Y_DRIVER_TYPE DRV8825
#define Z_DRIVER_TYPE ADRV8825
#define Z2_DRIVER_TYPE DRV8825
// #define E0_DRIVER_TYPE A4988
// #define E1_DRIVER_TYPE A4988
Motion section:
#define DISTINCT_E_FACTORS
// #define PRO_B_WITH_LEADSCREW
#if ENABLED(PRO_B_WITH_LEADSCREW) // M8 leadscrew version
#define DEFAULT_AXIS_STEPS_PER_UNIT { 78.74, 78.74, 400, 105 }
#else // M8 threaded rod version
#define DEFAULT_AXIS_STEPS_PER_UNIT { 157.48, 157.48, 5120, 105 }
#endif
#define AUTO_BED_LEVELING_BILINEAR
```

Modification for the GT2560 board:

The low-viscosity hydrogels may be more prone to flow or dripping, leading to serious challenges in accurate deposition on the substrate. It is crucial to precisely control the syringe pumps movements. The hydrogel will be extruded from the nozzle through the leadscrew motion. Consequently, calculating the appropriate number of steps is extremely important. Any small deviation from the fitting steps could cause either over-extrusion or under-extrusion of the low-viscosity hydrogel. Minor changes for the GT2560 main board are required to control the syringe pumps. FDM 3D printers are using commands that set the number of steps required for moving axes one millimeter. Based on the new configuration, it is more convenient to change this command by calculating the number of steps demanded for moving one milliliter. This can be done by determining the inner diameter of the syringe to calculate the plunger area. Then, the linear movement of the syringe to inject 1 ml can be calculated by: $\frac{1\text{cm}^3 / \text{Plungerarea} \text{cm}^2}{\text{Step_per_unit}}$ [24]. The calculated number can be inserted into the marlin firmware and then uploaded onto the main board.

```
#define DISTINCT_E_FACTORS
#define DEFAULT_AXIS_STEPS_PER_UNIT f { 61501.729, 61501.729, 61501.729, 5000 }
```

6. Operation instructions

6.1. Syringe pumps

To control the pumps, a computer should be connected to the board via USB cable and using open-source direct controlling software such as PronterFace (Fig. 16). Next, a G-code file is required to command the pumps and printer. G-Code is a set of commands which firmware executes line by line to operate the motors. The G-code can be written in a text editor and saved as “.gcode” or simply written in the allocated command prompt field in the PronterFace software. Few simple codes are required to control the pumps as follow:

- M302 S0**; this command leads to stop controlling for temperature and then cold extrusion can be possible.
- M211 S0**; this command will disable the end stops which might lead to problems since they are not connected.
- G91**; set the printer to relative positioning mode to avoid starting from 0.0, necessary for multiple movements.
- G1 X<ml> Y<ml> F<ml/min>**; to move the pumps for certain amount with specific flowrate.

6.2. 3D bioprinter

As previously mentioned, the 3D bioprinter and the syringe pumps are controlled by separate electronic boards, requiring separate G-code instructions to perform the printing process. The operation instructions for the printhead movement initiate by connecting the Rumba board to the PC with the USB cable. Next, the Repetier Host software (Fig. 17) must be opened in order to upload the specific gcode (Fig. 18). To this end, the connect button will be used to provide connection between the software and the device. Following this step, the home positioning should be done by simply pressing the home button. In the next step, the nozzle is inserted into the platform holder and the prepared gcode is loaded from the load section. After loading the gcode, the 3D bioprinter is ready to start the deposition process.

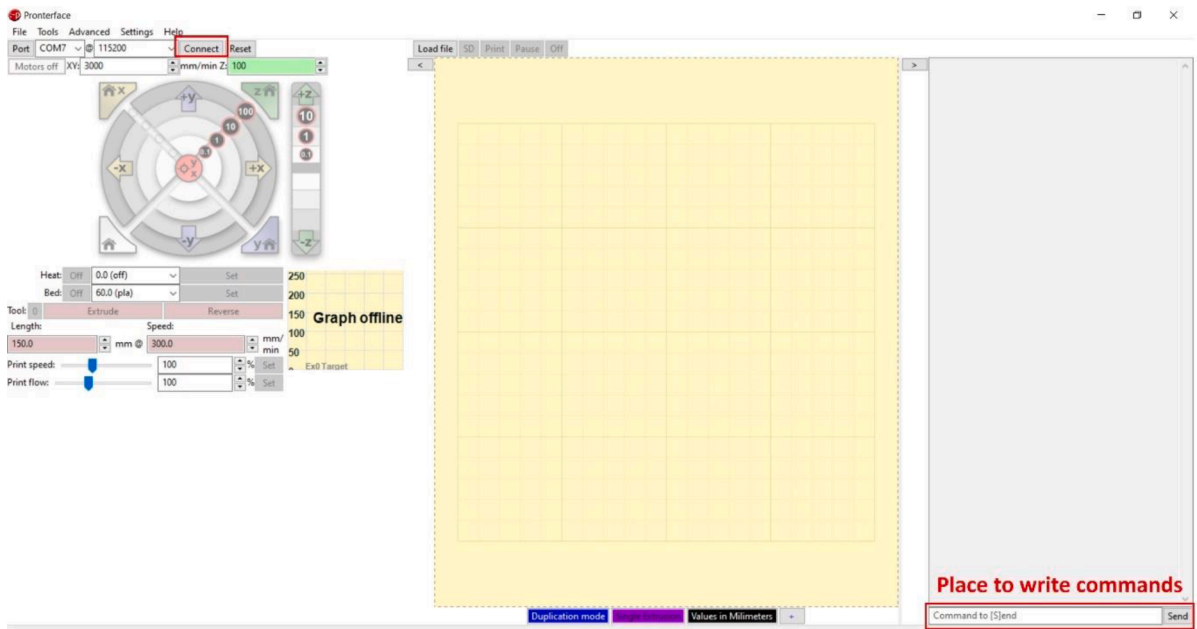


Fig. 16. PronterFace window and the injecting process from syringe pumps.

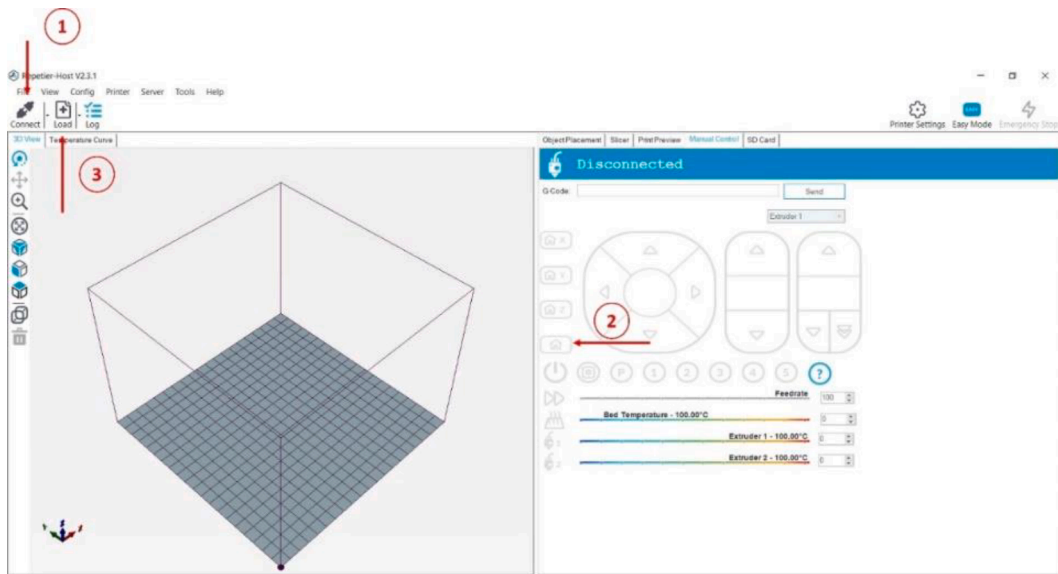


Fig. 17. Repetier Host window and the process involved in importing the G-code file.

7. Validation and characterization

To validate the performance of the MOS3S bioprinter, we have (i) investigated the accuracy of the syringe pumps in case of liquid delivery and (ii) printed a lattice scaffold with 4 % Alginate and 1.5 % Gelatin (AG) material ink.

7.1. Syringe pumps performance

To investigate the ability of the 3D microfluidic bioprinter to deliver with accuracy while minimizing the waste of materials by precise control over the dispensed amount, a series of liquid volumes were delivered ranging from 50 to 280 μ l. Each volume setting was repeated three times to ensure consistency. The collected amounts of deionized water have been measured using an analytical scale to determine the actual dispensed volume (Fig. 19a). To quantify the agreement between the programmed and actual delivered

```

1  G92 X0 Y0 Z10
2  G1 Z3.500 F650.000
3  G1 X10.000 F650.000
4  G3 Y1.000 I0 J0.500 F715.000
5  G1 X0 F650.000
6  G2 Y2.000 I0 J0.500 F715.000
7  G1 X10.000 F650.000
8  G3 Y3.000 I0 J0.500 F715.000
9  G1 X0 F650.000
10 G2 Y4.000 I0 J0.500 F715.000
11 G1 X10.000 F650.000
12 G3 Y5.000 I0 J0.500 F715.000
13 G1 X0 F650.000
14 G2 Y6.000 I0 J0.500 F715.000
15 G1 X10.000 F650.000
16 G3 Y7.000 I0 J0.500 F715.000
17 G1 X0 F650.000
18 G2 Y8.000 I0 J0.500 F715.000
19 G1 X10.000 F650.000
20 G3 Y9.000 I0 J0.500 F715.000
21 G1 X0 F650.000
22 G2 Y10.000 I0 J0.500 F715.000
23 G1 X10.000 F650.000

```

Fig. 18. Part of a G-code example for printhead movement in lattice scaffold deposition.

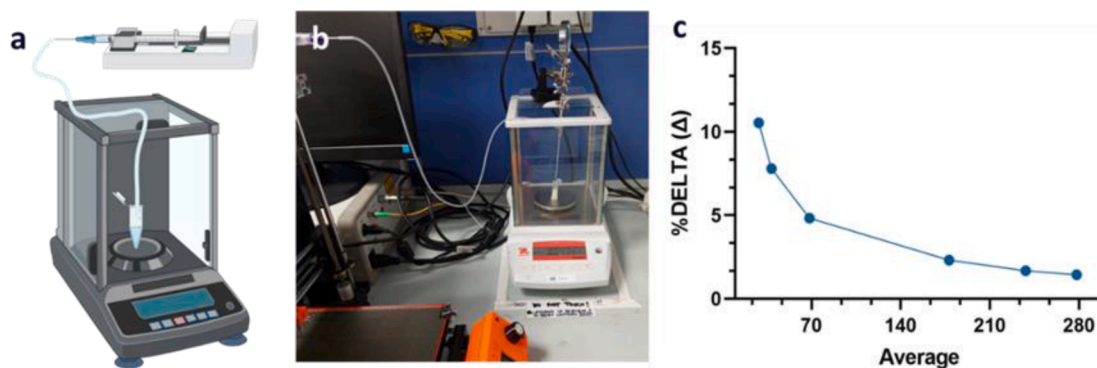


Fig. 19. (a) Schematic representation of the experimental set up. (b) Experimental set up to investigate the syringe pump accuracy. (c) Bland-Altman analysis to plot percentage difference between actual and theoretical volume.

volumes (Fig. 19b), a Bland-Altman analysis was performed in GraphPad Prism V9.0.0. As shown in Fig. 19c, the Bland-Altman plot displayed a clear pattern of the percentage difference between programmed and actual volumes decreased as the average volume increased. This trend is indicative of the syringe pumps' enhanced accuracy at higher volume settings.

7.2. Scaffold fabrication

A coaxial nozzle was prepared using 18G blunt needle as outer shell to guide CaCl_2 for *in situ* crosslinking and 25G blunt nozzle as inner core for the delivery of the composite material ink. The loaded syringes with material ink and crosslinking agent were placed on the custom-made 3D printed syringe pumps. Tygon tubes were used to transfer the material ink and crosslinking agent from the syringes to the microfluidic chip or coaxial nozzle for subsequent deposition on the pre-selected substrate. The mechanical and bioinert properties, as well as the possibility to sterilize the tubing by autoclaving make tygon tubing appropriate for proper flow of the ink during the printing process. The injection flowrate and printhead speed were set to $30 \mu\text{l}/\text{min}$ and $10.8 \text{ mm}/\text{s}$ with an acceleration rate to reach $11.9 \text{ mm}/\text{s}$ at the edges, respectively.

Hydrogel composites have shown stability and structural integrity under a range of temperatures [25]; making them suitable inks for printing at room temperature, without the need for precise temperature control. Thanks to microfluidic-assisted extrusion-based set-up and its capability to perform effectively at ambient temperature and typical laboratory conditions, the inks were prepared in the

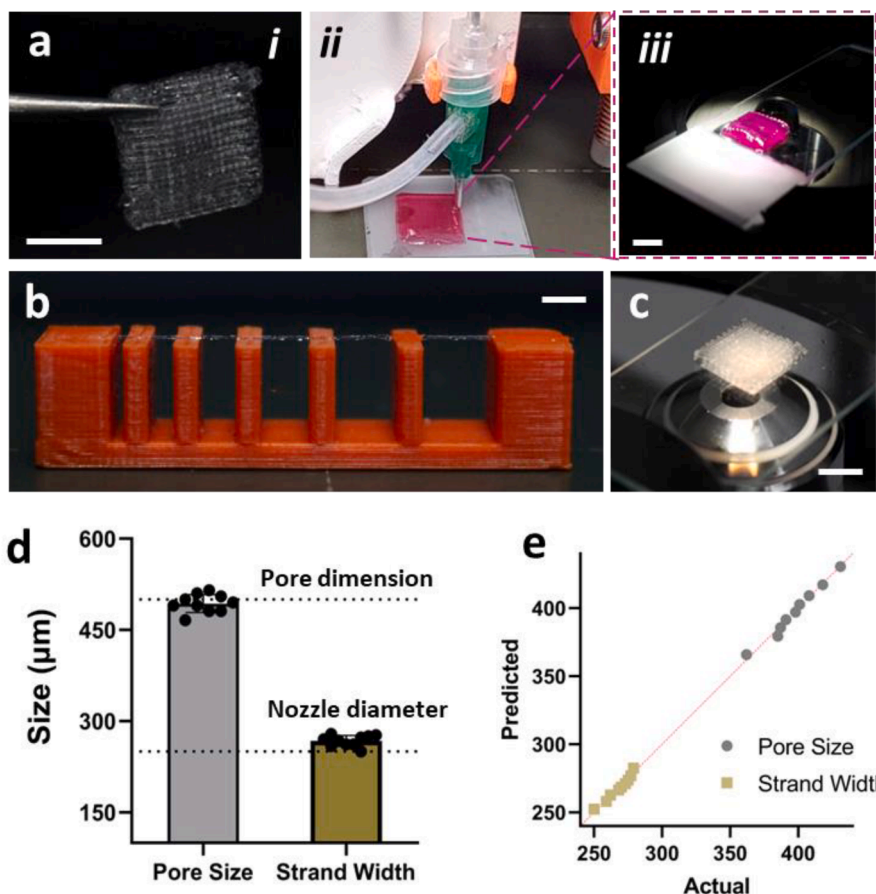


Fig. 20. (a) 3D biprinted scaffolds (i) label-free and (ii) rhodamine-labelled for (iii) imaging. (b) Collapse test performed on the pillar structures with increasing gap size to demonstrate ultimate (c) printability and printing resolution. (d) Pore size and strand width of printed scaffold compared to design. (e) Q-Q plot indicating the normality of the measurement. Scale bar is 5 mm.

liquid state while printing, where the temperature fluctuations had minimal impact on their rheological properties and the output quality.

To demonstrate the ability to produce three-dimensional scaffolds with accuracy and relevant for tissue engineering and regenerative medicine, we biprinted an 8-layer lattice grid structure with 500 μm pore size and filament width of 250 μm (Fig. 20a). The MOS3S platform has been developed from a desktop FDM 3D printer, without further axis modification. Thus, the resolution in all axes is in accord with the commercial extrusion-based systems. Therefore, the layer height for the printed scaffold was set to minimum of 200 μm . Standard filament collapse test (Fig. 20b) [26,27] revealed the ability of the microfluidic-assisted printer to generate free-standing fibers capable of holding their printed shape even over increasing support gaps. The combined ability to rapidly crosslink and deposit sub-millimeter fibers resulted in the fabrication of highly ordered scaffolds (Fig. 20c).

The physical characterization of the scaffolds performed with image processing software (ImageJ), revealed high resolution and printing accuracy of the fabricated constructs. Pore size and strand width (Fig. 20d) were measured and found to be non-significantly different from the blueprint, confirming the 3D biprinter high-end resolution. A further analysis over the distribution of the observed dataset revealed in a Q-Q plot (Fig. 20e) the minimal deviation from the 45-degree interpolation, suggesting a negligible difference with the theoretical normal distribution of the measurements. This ultimately confirmed the ability of the 3D microfluidic biprinter to deliver high-resolution constructs.

To demonstrate the versatility of MOS3S, we engineered a library of polymer composites that can result printable by the microfluidic-based 3D biprinting system here proposed (Fig. 21). The printed scaffolds encompass various compositions, including different percentages of alginate, gelatin methacryloyl (GelMA), Hyaluronic Acid (HA), laponite, and chitosan, thereby illustrating the system's broad applicability across a range of biomaterial formulations. The library was designed to demonstrate the printing of low-viscosity hydrogels while maintaining elevated resolution for a 3D biprinting system. Indeed, we demonstrated that the inclusion of a small percentage of Laponite (Fig. 21 c) allowed for a significant improvement in printing accuracy (Fig. 21d) as previously reported [28]. The inclusion of natural polymers blended with alginate, did not result in a significant difference in printing resolution (Fig. 21h).

Employing multiple syringe pumps will enable the users to deposit multiple materials for fabricating hierarchical scaffolds. This multiple material could either have different formulation, or the agents encapsulated within the hydrogel. In Fig. 22, we investigated

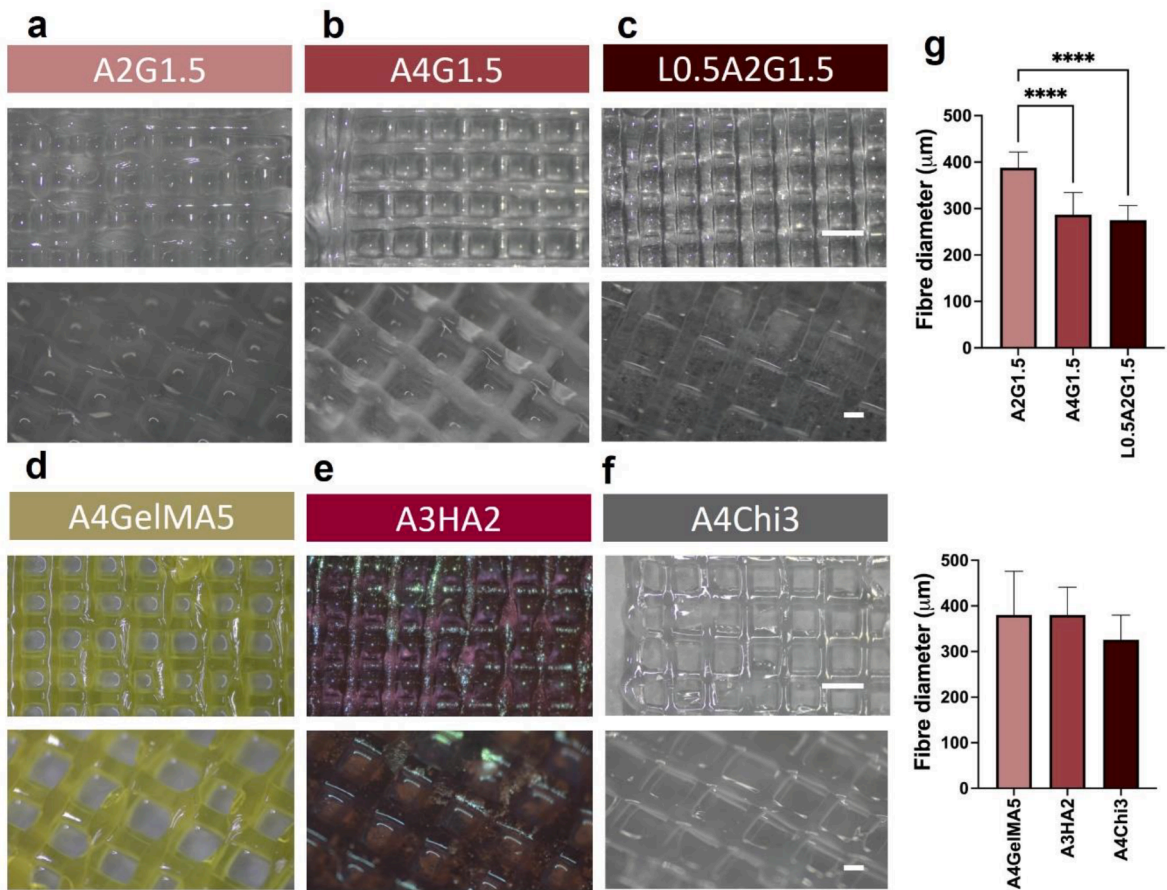


Fig. 21. A library of printed hydrogel biomaterials with different range of viscosity. (a) Alginate 2% Gelatine 1.5%, (b) Alginate 4% Gelatin 1.5%, (c) Laponite 0.5% Alginate 2% Gelatin 1.5%, (d) Alginate 4% GelMA 5%, (e) Alginate 3% Hyaluronic Acid (HA) 2%, (f) Alginate 4% Chitosan 3% and (g) characterization of the printed scaffolds. Scale bars: 1 mm.

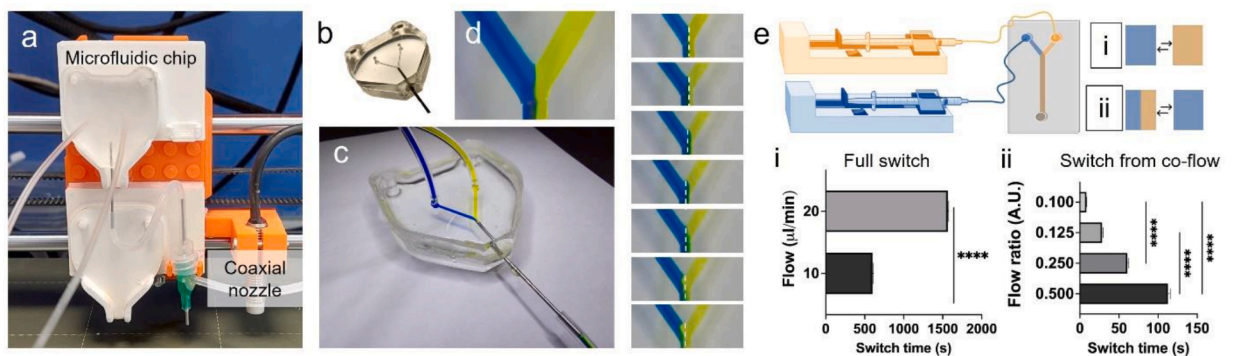


Fig. 22. (a) Macrographs of the connection between the microfluidic chip and the coaxial nozzle. (b) Microfluidic chip printhead realized in polydimethylsiloxane (PDMS) and the metal needle for injection. (c) Transferring the labelled fluids into the microfluidic chip. (d) Close view of the distribution of blue and yellow fluids and transition progress upon adjusting the flow of the syringes. (e) Schematic diagram of the syringes set-up and quantification on the system's performance in (i) full (0 to 100%) and (ii) partial (50% to 100%) transition study. (For interpretation of the references to color in this figure legend, the reader is referred to the web version of this article.)

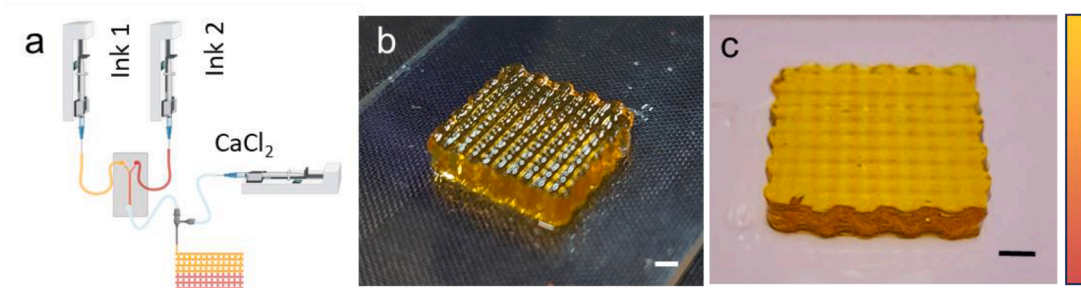


Fig. 23. (a) Schematic representation of the process for fabricating graded scaffolds. (b) Side and (c) view of the 20-layer scaffold with gradient pattern. Scale bar is 2 mm.

the switching dynamics between two inks within the microchannels. Fig. 22(a) depicts the experimental setup, consisting of the microfluidic channel mixer attached to the coaxial nozzle and printhead. Our study evaluated the efficacy of the microfluidic-assisted extrusion-based bioprinting system in transitioning between different labelled inks, both completely (from 0 to 100 % of flow rate) and partially (from 50 % - co-flow – to 100 % of flow rate). The results of our study indicate that the transition from 0 % to 100 % ink takes approximately 8 min at a flow rate of 20 $\mu\text{l}/\text{min}$ and 16 min at a flow rate of 10 $\mu\text{l}/\text{min}$.

To demonstrate the ability of the new custom-made MOS3S to deliver graded structures in a continuous fashion in a single construct, we engineered a gradient of color-tagged (red and yellow) AG material inks (Fig. 23a), resulting in similar rheology, viscosity and mechanical properties. The 3D lattice construct was layered up to 20 layers to reach a consistent graded transition from red to yellow over the full Z-height (Fig. 23b). This feature implemented with our MOS3S bioprinter can be customized to replicate multi-gradient structures and deliver a variety of growth factors or cells in 3D to engineer more complex functional tissue substitutes. However, it is noteworthy to mention that, if the used inks in each syringe are vastly different in terms of viscosity, some adjustments may be required to minimize potential issues arising from this misalignment. The utmost challenge while depositing multiple materials is to have timing and precise GCode to initiate the flow of the second material ink when the preceding ink is dispensed. This would result in the minimum interruption and ensures the smooth extrusion of the inks. Further use of mixing chip printheads are currently under investigation and will be object of further studies.

Furthermore, multiple tissue engineering applications can span from this customized system. For instance, the microfluidics-assisted extrusion-based system in our bioprinter could support real-time mixing of inks, enabling the development of gradient structures and composite materials with customized characteristics.

In summary, we demonstrated the successful development of a novel open-source and low-cost microfluidic-assisted extrusion-based 3D bioprinter (MOS3S) which can be assembled with limited efforts and low-budget (< €700), to be used in a variety of applications including the hierarchical patterning of biomaterial inks of interests, high-resolution 3D bioprinting and gradient constructs fabrication. The flexibility of our systems allows for further modifications such as the inclusion of an increasing number of syringe pumps for more complex studies. Nevertheless, printing accuracy can be further implemented to support the printing process with an on-the-fly (i) Z-height calibration and (ii) X-Y speed control. Further implementations are under investigation and object of further studies.

Overall, the custom 3D microfluidic-assisted bioprinter demonstrates great promise to be used in the field of tissue engineering to produce constructs for further tissue repair, disease modeling or drug discovery.

CRediT authorship contribution statement

Sajad Mohammadi: Writing – original draft, Visualization, Validation, Methodology, Data curation, Conceptualization. **Salvatore D’Alessandro:** Writing – original draft, Validation, Methodology, Formal analysis, Data curation, Conceptualization. **Fabiano Bini:** Supervision, Software, Resources, Project administration. **Franco Marinozzi:** Supervision, Software, Resources, Project administration. **Gianluca Cidonio:** Writing – review & editing, Writing – original draft, Visualization, Validation, Supervision, Resources, Project administration, Methodology, Funding acquisition, Conceptualization.

Declaration of competing interest

The authors declare that they have no known competing financial interests or personal relationships that could have appeared to influence the work reported in this paper.

Acknowledgments

The authors would like to thank the entire 3D microfluidic biofabrication lab (IIT), Prof Andrea Barbetta and Mr Giorgio Amico (University of Rome La Sapienza) for the useful discussions, support and insight in the further development of the presented apparatus.

Human and animal

The work did not involve human or animal subjects.

Appendix A. Supplementary data

Supplementary data to this article can be found online at <https://doi.org/10.1016/j.ohx.2024.e00527>.

References

- [1] G. Cidonio, M. Costantini, F. Pierini, C. Scognamiglio, T. Agarwal, A. Barbetta, 3D printing of biphasic inks: beyond single-scale architectural control, *J. Mater. Chem. C* 9 (2021) 12489–12508, <https://doi.org/10.1039/D1TC02117F>.
- [2] E. Demircan, B. Özçelik, Development of affordable 3D food printer with an exchangeable syringe-pump mechanism, *HardwareX* 14 (2023) e00430, <https://doi.org/10.1016/j.ohx.2023.e00430>.
- [3] N. Shahrubudin, T.C. Lee, R. Ramlan, An overview on 3D printing technology: technological, materials, and applications, *Procedia Manuf.* 35 (2019) 1286–1296, <https://doi.org/10.1016/j.promfg.2019.06.089>.
- [4] D. van der Heide, G. Cidonio, M.J. Stoddart, M. D'Este, 3D printing of inorganic-biopolymer composites for bone regeneration, *Biofabrication* 14 (2022) 042003, <https://doi.org/10.1088/1758-5090/ac8cb2>.
- [5] L. Iafate, M.C. Benedetti, S. Donsante, A. Rosa, A. Corsi, R.O.C. Oreffo, M. Riminucci, G. Ruocco, C. Scognamiglio, G. Cidonio, Modelling skeletal pain harnessing tissue engineering, *Vitro Models* 1 (2022) 289–307, <https://doi.org/10.1007/s44164-022-00028-7>.
- [6] K. Kumar, D. Zindani, J.P. Davim, (Eds.), *Additive Manufacturing Technologies From an Optimization Perspective*, IGI Global, 2019. <https://doi.org/10.4018/978-1-5225-9167-2>.
- [7] R. Levato, O. Dudaryeva, C.E. Garciamendez-Mijares, B.E. Kirkpatrick, R. Rizzo, J. Schimelman, K.S. Anseth, S. Chen, M. Zenobi-Wong, Y.S. Zhang, Light-based vat-polymerization bioprinting, *Nat. Rev. Methods Primer* 3 (2023) 47, <https://doi.org/10.1038/s43586-023-00231-0>.
- [8] C. Scognamiglio, A. Soloperto, G. Ruocco, G. Cidonio, Bioprinting stem cells: building physiological tissues one cell at a time, *Am. J. Physiol.-Cell Physiol.* 319 (2020) C465–C480, <https://doi.org/10.1152/ajpcell.00124.2020>.
- [9] S. Ramesh, O.L.A. Harrysson, P.K. Rao, A. Tamayol, D.R. Cormier, Y. Zhang, I.V. Rivero, Extrusion bioprinting: Recent progress, challenges, and future opportunities, *Bioprinting* 21 (2021) e00116, <https://doi.org/10.1016/j.bprint.2020.e00116>.
- [10] E. Davoodi, E. Sarikhani, H. Montazerian, S. Ahadian, M. Costantini, W. Świeżkowski, S.M. Willerth, K. Walus, M. Mofidfar, E. Toyserkani, A. Khademhosseini, N. Ashammakhi, Extrusion and microfluidic-based bioprinting to fabricate biomimetic tissues and organs, *Adv. Mater. Technol.* 5 (2020) 1901044, <https://doi.org/10.1002/admt.201901044>.
- [11] N. Bessler, D. Ogiermann, M.-B. Buchholz, A. Santel, J. Heidenreich, R. Ahmed, H. Zaehres, B. Brand-Saberi, Nydus One Syringe Extruder (NOSE): A Prusa i3 3D printer conversion for bioprinting applications utilizing the FRESH-method, *HardwareX* 6 (2019) e00069, <https://doi.org/10.1016/j.ohx.2019.e00069>.
- [12] M. Marcotulli, M.C. Tirelli, M. Volpi, J. Jaroszewicz, C. Scognamiglio, P. Kasprzycki, K. Karnowski, W. Świeżkowski, G. Ruocco, M. Costantini, G. Cidonio, A. Barbetta, Microfluidic 3D printing of emulsion ink for engineering porous functionally graded materials, *Adv. Mater. Technol.* 8 (2023) 2201244, <https://doi.org/10.1002/admt.202201244>.
- [13] S. Mohammadi, G. Cidonio, Unravelling hierarchical patterning of biomaterial inks with 3D microfluidic-assisted spinning: a paradigm shift in bioprinting technologies, *Front. Biomater. Sci.* 2 (2023) 1279061, <https://doi.org/10.3389/fbiom.2023.1279061>.
- [14] Y. He, Y. Wu, J. Fu, Q. Gao, J. Qiu, Developments of 3D printing microfluidics and applications in chemistry and biology: a review, *Electroanalysis* 28 (2016) 1658–1678, <https://doi.org/10.1002/elan.201600043>.
- [15] M. Mohamed, H. Kumar, Z. Wang, N. Martin, B. Mills, K. Kim, Rapid and inexpensive fabrication of multi-depth microfluidic device using high-resolution LCD stereolithographic 3D printing, *J. Manuf. Mater. Process.* 3 (2019) 26, <https://doi.org/10.3390/jmmp3010026>.
- [16] D.N. Du Chatinier, K.P. Figler, P. Agrawal, W. Liu, Y.S. Zhang, The potential of microfluidics-enhanced extrusion bioprinting, *Biomicrofluidics* 15 (2021) 041304, <https://doi.org/10.1063/5.0033280>.
- [17] F. Koch, O. Thaden, K. Tröndle, R. Zengerle, S. Zimmermann, P. Koltay, Open-source hybrid 3D-bioprinter for simultaneous printing of thermoplastics and hydrogels, *HardwareX* 10 (2021) e00230, <https://doi.org/10.1016/j.ohx.2021.e00230>.
- [18] J.W. Tashman, D.J. Shiwarski, A.W. Feinberg, A high performance open-source syringe extruder optimized for extrusion and retraction during FRESH 3D bioprinting, *HardwareX* 9 (2021) e00170, <https://doi.org/10.1016/j.ohx.2020.e00170>.
- [19] M. Kahl, M. Gertig, P. Hoyer, O. Friedrich, D.F. Gilbert, Ultra-low-cost 3D bioprinting: modification and application of an off-the-shelf desktop 3D-printer for biofabrication, *Front. Bioeng. Biotechnol.* 7 (2019) 184, <https://doi.org/10.3389/fbioe.2019.00184>.
- [20] B. Yenilmez, M. Temirel, S. Knowlton, E. Lepowsky, S. Tasoglu, Development and characterization of a low-cost 3D bioprinter, *Bioprinting* 13 (2019) e00044, <https://doi.org/10.1016/j.bprint.2019.e00044>.
- [21] Q. Li, L. Ma, Z. Gao, J. Yin, P. Liu, H. Yang, L. Shen, H. Zhou, Regulable supporting baths for embedded printing of soft biomaterials with variable stiffness, *ACS Appl. Mater. Interfaces* 14 (2022) 41695–41711, <https://doi.org/10.1021/acsami.2c09221>.
- [22] D. Chimene, K.A. Deo, J. Thomas, A.K. Gaharwar, Designing cost-effective, open-source, multi-head bioprinters via conversion of hobby-grade 3D printers, *Bioengineering* (2022), <https://doi.org/10.1101/2022.03.24.483055>.
- [23] MarlinFirmware, Home, Marlin Firmware. (n.d.), Marlin Firmware (n.d.). <https://marlinfw.org/> (accessed May 31, 2021).
- [24] S. Baas, V. Saggiomo, Ender3 3D printer kit transformed into open, programmable syringe pump set, *HardwareX* 10 (2021) e00219, <https://doi.org/10.1016/j.ohx.2021.e00219>.
- [25] A.C. Dell, G. Wagner, J. Own, J.P. Geibel, 3D bioprinting using hydrogels: cell inks and tissue engineering applications, *Pharmaceutics* 14 (2022) 2596, <https://doi.org/10.3390/pharmaceutics14122596>.

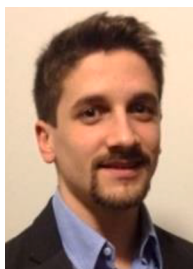
- [26] J.M. Rodríguez-Rego, L. Mendoza-Cerezo, A. Macías-García, J.P. Carrasco-Amador, A.C. Marcos-Romero, Methodology for characterizing the printability of hydrogels, *Int. J. Bioprint.* 9 (2023), <https://doi.org/10.18063/ijb.v9i2.667>.
- [27] A. Ribeiro, M.M. Blokzijl, R. Levato, C.W. Visser, M. Castilho, W.E. Hennink, T. Vermonden, J. Malda, Assessing bioink shape fidelity to aid material development in 3D bioprinting, *Biofabrication* 10 (2017) 014102, <https://doi.org/10.1088/1758-5090/aa90e2>.
- [28] Y.-H. Kim, J.M. Kanczler, S. Lanham, A. Rawlings, M. Roldo, G. Tozzi, J.I. Dawson, G. Cidonio, R.O.C. Oreffo, Biofabrication of nanocomposite-based scaffolds containing human bone extracellular matrix for the differentiation of skeletal stem and progenitor cells, *Bio-Des. Manuf.* (2024), <https://doi.org/10.1007/s42242-023-00265-z>.



Sajad Mohammadi Master of Science (MSc) in Nanotechnology Engineering graduated from Sapienza University of Rome, Italy with a focus on tissue engineering and microfluidic 3D bioprinting. At the moment of this project, he was a thesis student at the Microfluidic 3D Bioprinting Lab (3DMB Lab), Center for Life Nano & Neuroscience (CLN2S), Italian Institute of Technology (IIT).



Salvatore Alessandro Ph.D. student in Biomedical Engineering at the Department of Biomedical Engineering, Sapienza University of Rome and 3DMB Lab, CLN2S, Italian Institute of Technology. His focus is on irregular scaffold fabrication using novel additive manufacturing techniques such as 3D printing and robotic arms.



Gianluca Cidonio Graduated (BSc and MSc) in Biomedical Engineering from Sapienza University of Rome, Italy, and Ph.D. from Bone and Joint Research Group, University of Southampton, UK. He joined the Center for Life Nano- & Neuro- Science (CLN²S) in IIT as a research scientist in 2019, to work on novel microfluidic-bioprinting technology for the fabrication of complex and physiological tissue substitutes.